JACS
JOURNAL OF THE AMERICAN CHEMICAL SOCIETY
Communication
pubs.acs.org/JACS

Organic Radical Contrast Agents for Magnetic Resonance Imaging

Andrzej Rajca,*[,†] Ying Wang,[†] Michael Boska,[‡] Joseph T. Paletta,[†] Arnon Olankitwanit,[†] Michael A. Swanson,[§] Deborah G. Mitchell,[§] Sandra S. Eaton,[§] Gareth R. Eaton,[§] and Suchada Rajca[†]

[†]Department of Chemistry, University of Nebraska, Lincoln, Nebraska 68588-0304, United States
[‡]Department of Radiology, University of Nebraska Medical Center, Omaha, Nebraska 68198, United States
[§]Department of Chemistry and Biochemistry, University of Denver, Denver, Colorado 80208-2436, United States

Supporting Information

ABSTRACT: We report a molecular design that provides an intravenously injectable organic radical contrast agent (ORCA) for which the molecular ^{1}H water relaxivity (r_1) is ca. 5 mM^{-1} s^{-1}. The ORCA is based on spirocyclohexyl nitroxide radicals and poly(ethylene glycol) chains conjugated to a fourth-generation polypropylenimine dendrimer scaffold. The metal-free ORCA has a long shelf life and provides selectively enhanced magnetic resonance imaging in mice for over 1 h.

Paramagnetic organic radicals, such as stable nitroxides, have been investigated as magnetic resonance imaging (MRI) contrast agents.[1−6] Metal-free organic radical contrast agents (ORCAs) would provide an alternative to gadolinium-based contrast agents (GBCAs), which are the most widely used paramagnetic metal ion-based agents in the clinic. Although GBCAs are well-tolerated by the majority of patients, patients with impaired kidney function are reported to have increased risk of developing a serious adverse reaction named nephrogenic systemic fibrosis (NSF).[7] Since the first report of this adverse effect in renal dialysis patients and its association with gadolinium,[8,9] guidelines for the administration of GBCAs have been issued and implemented worldwide to minimize the risk of NSF.

To date, the critical obstacle in the development of practical ORCAs for MRI is the design and synthesis of paramagnetic compounds of moderate molecular size that possess long in vivo lifetimes, high ^{1}H water relaxivities (r_1), and high water solubility.[1−6]

Commonly-used paramagnetic nitroxides undergo fast reduction in vivo, especially in the bloodstream and tissues, to form diamagnetic hydroxylamines.[2,3] For example, 3-carboxy-2,2,5,5-tetramethyl-l-pyrrolidinyloxy (3-CP) (see Scheme 1) and its derivatives, which are among the most widely used and reduction-resistant nitroxide radicals, have a short half-life (ca. 2 min) in the bloodstream and kidneys, as determined by MRI mouse studies.[2,3] Although nitroxides with one unpaired electron [total spin quantum number (S) = $^1/_2$] possess low ^{1}H water relaxivities[10] (e.g., $r_1 \approx 0.15$ mM^{-1} s^{-1} at 7 T for 3-CP), they have been utilized as functional redox-sensitive agents in MRI studies and as in vivo radio-protectors.[2,3,11] In principle, r_1 could be increased by conjugation of paramagnetic metal chelates or radicals to rigid scaffolds.[12−14] However, previous examples of conjugation of nitroxides to dendrimers did not provide increased r_1,[15,16] as shown in the case of the third-generation (G3) polypropylenimine (PPI) dendrimers conjugated with 3-CP, for which $r_1 \approx 0.16$ mM^{-1} s^{-1} at 1.5 T, similar to that for common nitroxides. Despite their low r_1 and low solubility in water,[15] in vivo MR images of rabbit stifle joints obtained by intraarticular administration of these agents showed significant enhancement of articular cartilage in T_1-weighted images.[1] The fast reduction and low r_1 of nitroxides pose serious obstacles because they severely limit the available MRI time and contrast, and increasing the dose of the agent to compensate for the reduction and low r_1 could lead to oxidative stress.[17] A practical ORCA, especially suitable for intravenous injection, remains elusive. Herein we report a water-soluble ORCA with a long in vivo lifetime and high r_1 that provides selectively enhanced MRI in mice for over 1 h.

Our approach to ORCA design (Figure 1) relies on the spirocyclohexyl nitroxide radical **1**-OH. The five-membered-

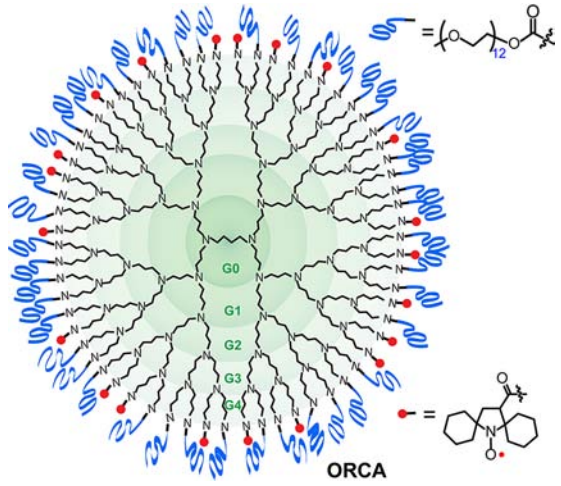

Figure 1. Organic radical contrast agent (ORCA).

ring (pyrrolidinyl) nitroxide radical[18,19] that is sterically shielded[20] by the spirocyclohexyl groups[21] would be expected to be reduced at a lower rate in vivo, particularly by antioxidants such as ascorbate (vitamin C). Through judicious molecular design, conjugation of nitroxide radicals to a rigid

Received: August 10, 2012
Published: September 13, 2012

   dx.doi.org/10.1021/ja3079829 | J. Am. Chem. Soc. 2012, 134, 15724−15727

scaffold should provide an agent with not only increased resistance to reduction but also with increased relaxivity. We considered dendrimers (branched structures), which have been demonstrated to be more effective than linear structures as scaffolds for linking Gd chelates in approaches leading to GBCAs with increased relaxivity.[13,14,22] Because the hydrophobicity of the surface of the nitroxide-covered dendrimer may contribute to limited applications of the agents in MRI, our approach aimed to alleviate that effect by including water-solubilizing groups such as poly(ethylene glycol) (PEG) chains on the surface of the dendrimer. The nonimmunogenic and polar PEG chains may provide additional advantages,[23] such as helping to immobilize the nitroxides and increasing water access to the paramagnetic nitroxides, which could help to increase r_1. Our design strategy involved optimizing the ratio of nitroxide and PEG chains on the dendrimer surface to obtain an ORCA with high r_1 and good water solubility. This concept was tested using PPI dendrimers conjugated with spirocyclohexyl nitroxide **1** and hydrophilic, monodisperse methoxy-PEG (mPEG-12) chains to obtain a water-soluble ORCA.

Spirocyclohexyl nitroxide **1**-OH was synthesized by modification of methods for 3-CP,[24] and then the carboxylic acid was converted to *N*-hydroxysuccinimidyl (NHS) ester **1**-NHS using standard methods (Scheme 1). Sequential conjugation of

Scheme 1

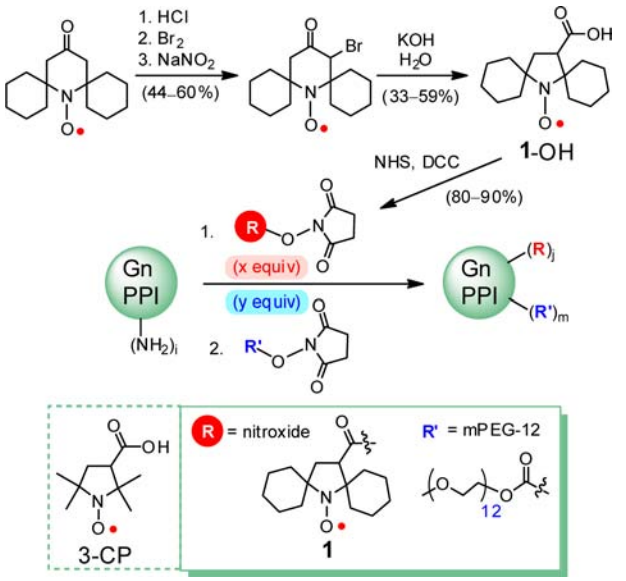

1-NHS and mPEG-12-NHS to the fourth-generation PPI dendrimer (PPI-G4) with 64 terminal amine groups [$(NH_2)_i$, i = 64] provided ORCA **1**-mPEG-G4. Through tests of various reaction conditions, it was determined that using $^1/_3$ equiv of **1**-NHS and more than $^2/_3$ equiv of mPEG-NHS is optimum. The resultant **1**-mPEG-G4 has a water solubility of ≥0.5 g/mL and a radical concentration of ≥0.4 mmol/g. The ORCAs **1**-mPEG-G3, **1**-mPEG-G2, and **1**-mPEG-G0 as well as 3-CP-mPEG-G4 were prepared by analogous procedures (see Table 1).

The number of conjugated spirocyclohexyl nitroxide **1** and mPEG-12 moieties per PPI dendrimer core was determined using end-group analysis based upon ^{1}H NMR spectroscopy and spin counting by electron paramagnetic resonance (EPR) spectroscopy. Because the ^{1}H NMR spectra of paramagnetic ORCAs are broad and not useful for characterization, we converted the nitroxides to diamagnetic hydroxylamines by treating the ORCAs with an excess of ascorbate. The partially reduced ORCAs provided sufficiently well resolved ^{1}H NMR spectra that permit the number of conjugated mPEG-12 moieties (m) to be determined by the relative integrals of the ^{1}H resonances for the terminal methyl groups of mPEG-12 and the ^{1}H resonances of the dendrimer scaffold. Spin counting provided the spin concentration of the ORCA sample (prior to treatment with ascorbate), which was used to determine the number of conjugated nitroxide radicals (j). The PPI dendrimer surface coverages determined from the values of m and j are shown in Table 1. For **1**-mPEG-G4, ca. 80% of the dendrimer surface was covered with nitroxides **1** and mPEG-12, and this surface coverage increased to ca. 90% for lower-generation ORCAs. This incomplete surface coverage may be associated with the well-known overcrowding on the surfaces of the higher-generation dendrimers,[25] which is further amplified by the larger space requirements of **1** versus mPEG-12, as illustrated by the surface coverages of 64 and 92% for the model compounds **1**-G4 and mPEG-G4. Covalent attachment of both mPEG-12 and the reduced nitroxides (hydroxylamines) to the scaffold was evidenced by two broad ^{1}H NMR peaks at 7.9 and 10.4 ppm (dimethyl sulfoxide-d_6), assigned to two distinct NH amide groups. mPEG-G4 has only one type of NH amide group (a singlet at 7.9 ppm), which showed a ^{1}H–^{1}H correlation spectroscopy (COSY) cross-peak to the dendrimer backbone [Figures S10–S18 in the Supporting Information (SI)].

We investigated the rate of reduction of nitroxides **1**-OH and ORCA **1**-mPEG-G4 under pseudo-first-order conditions using a 20-fold excess of ascorbate in pH 7.4 phosphate-buffered saline (PBS). As a reference, the rate of reduction of 3-CP was determined under identical conditions. Second-order rate constants, k, were obtained by following the decay of the nitroxide EPR peak height at 295 K (Figure 2A). The spirocyclohexyl nitroxide, **1**-OH (k = 0.031 ± 0.003 M^{-1} s^{-1}) was reduced at a significantly lower rate than 3-CP (k = 0.063 ± 0.002 M^{-1} s^{-1}).[19] Under similar conditions, initial reduction of **1**-mPEG-G4 occurred with k = 0.058 ± 0.004 M^{-1} s^{-1}, which is comparable to that of 3-CP. However, after a fraction of the nitroxides was reduced during the initial 1 h period, the remaining nitroxides **1** on the crowded dendrimer surface were reduced at a ca. 20-fold lower rate (Table S2 in the SI).

The ^{1}H water relaxivities r_1 of the ORCAs and 3-CP in PBS were measured using a 7 T MRI scanner. The plots of the reciprocal of the ^{1}H relaxation rate of water ($1/T_1$) versus the nitroxide concentration were linear for all of the agents, indicating the absence of aggregation over the concentration range studied (0–16 mM per nitroxide) (Figure 2B). The slopes of the plots indicated that under physiological conditions (PBS, pH 7.2), the ^{1}H water relaxivities of PEGylated ORCAs are significantly higher than for 3-CP. For example, r_1 = 0.42 ± 0.03 mM^{-1} s^{-1} per S = $^1/_2$ nitroxide radical in **1**-mPEG-G4, corresponding to a molecular relaxivity of $r_1 \approx 5$ mM^{-1} s^{-1}, which may be compared with the value of $r_1 \approx 0.14$ mM^{-1} s^{-1} for 3-CP (Table 1). Solutions of **1**-mPEG-G4 in PBS were stable at room temperature, with r_1 showing negligible changes over 24 h; similarly, no change in the spin concentration was detected by EPR spectroscopy for **1**-mPEG-G4 in PBS stored at −20 °C for 5 months.

We examined the rotational dynamics of the ORCAs by EPR line-shape analysis. Because a high spin concentration leads to exchange broadening of EPR spectra, we decreased the spin

dx.doi.org/10.1021/ja3079829 | J. Am. Chem. Soc. 2012, 134, 15724–15727

Table 1. Summary of ORCAs[a]

PPI	i	ORCA	x (equiv)	y (equiv)	spin conc. (mmol g^{-1})	r_1 (mM^{-1} s^{-1})	τ_{rot} (ns)	j	m	m/j	surface coverage (%)	M_n (kDa)
G4	64	**1**-mPEG-G4	21−22	54−65	0.41 ± 0.01	0.42 ± 0.03	1.5 ± 0.1	13.1 ± 0.5	37.9 ± 2.0	2.90 ± 0.04	79.6 ± 4.0	32
G3	32	**1**-mPEG-G3	11	25	0.46 ± 0.01	0.37 ± 0.02	0.84 ± 0.06	8	20	2.5	86	17
G2	16	**1**-mPEG-G2	6	15	0.46 ± 0.04	0.29 ± 0.02	0.49 ± 0.02	4	10	2.5	90	8.4
G4	64	**1**-G4	70−80	0	2.36 ± 0.03	–	–	41 ± 1	0	0	64 ± 2	17
		mPEG-G4	0	70	0	–	–	0	59	–	92	41
		3-CP-mPEG-G4	21	52	0.50 ± 0.05	0.33	0.85 ± 0.07	–	–	–	–	–
		3-CP	–	–	–	0.14	~0.04	–	–	–	–	–

[a] r_1 (mM^{-1} s^{-1}): mM^{-1} of $S = {}^1/_2$ nitroxide radicals (per $S = {}^1/_2$ nitroxide radical); i is the number of NH_2 groups; x and y are molar equivalents of nitroxide-NHS and mPEG-12-NHS; j and m are the numbers of conjugated nitroxide radicals (R) and mPEG-12 moieties (R′) (see Scheme 1).

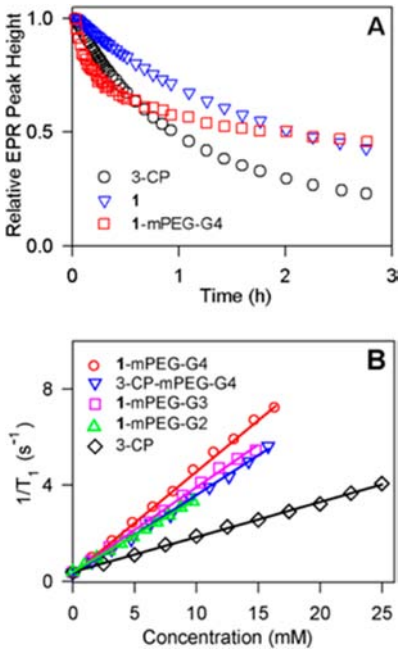

Figure 2. (A) Reduction of 0.2 mM nitroxide radicals with 4 mM ascorbate in 125 mM PBS (pH 7.4) at 295 K. (B) Plots of water ^{1}H relaxation rates, $1/T_1$, vs concentration of nitroxide radicals in PBS (pH 7.2); the water relaxivities r_1 were determined from the slopes of the linear fits (R^2 = 0.998−0.999).

concentration of the ORCAs by treatment with ascorbate in PBS to obtain adequately resolved EPR spectra for the analysis. Simulations of the EPR spectra of the partially reduced ORCAs provided rotational correlation times (τ_{rot}) in the nanosecond range (Table 1), compared with $\tau_{rot} \approx 0.04$ ns for 3-CP under identical conditions. The value of τ_{rot} for **1**-mPEG-G4 is ca. 50% longer than that for 3-CP-mPEG-G4, emphasizing the effectiveness of the more rigid spirocyclohexyl structure of nitroxide **1** in restricting the motion of the radical. Although the ORCA with the longest τ_{rot} (1.5 ± 0.1 ns) possesses the highest r_1, the relaxivity is only weakly dependent on τ_{rot}. This suggests the possibility that different factors limit r_1 for the ORCAs, such as a short electron spin relaxation time (T_{1e}) and a long residence/exchange time (τ_{exch}) of water molecules hydrogen-bonded to the nitroxide radical.

EPR line-shape analyses for **1**-mPEG-G4, -G3, and -G2 suggested that T_{1e} is longer than ca. 20 ns on the basis of the assumption that T_{1e} is greater than T_{2e} estimated from line widths. Because the dominant mechanism for shortening of T_{1e} is the modulation of electron−electron spin−spin interactions by motion,[26] the highly restricted motion of the radicals in the ORCAs ($\tau_{rot} \approx 1$ ns) is likely to prevent T_{1e} from becoming sufficiently short to affect the water r_1 significantly (Figure S22). This leaves long τ_{exch} as the most probable factor limiting the water r_1, similar to the behavior observed in conjugates of Gd chelates with dendrimers.[27] The dipolar inner-sphere model,[28] which is the standard in the analysis of Gd chelates,[13,22] predicts that shortening τ_{exch} to ≤1 μs (i.e., improved access of water to radicals) should facilitate increased water r_1. For example, the value $r_1 \approx 5$ mM^{-1} s^{-1} per $S = {}^1/_2$ nitroxide radical was computed for $\tau_{exch} \approx 1$ μs, $\tau_{rot} \approx 1.5$ ns, and $T_{1e} \geq 20$ ns (Figure S22).

To explore the potential of ORCAs as practical MRI contrast agents, we investigated **1**-mPEG-G4 in vivo. Since the value of r_1 per $S = {}^1/_2$ nitroxide radical for **1**-mPEG-G4 is ca. 3 times higher than for a typical nitroxide, we used a relatively small dose of radical, 0.5 mmol/kg, which is 3 times less than the typical dose for common nitroxides in in vivo MRI studies.[2,3] The T_1-weighted high-resolution 3D images of the mouse torso showed that the **1**-mPEG-G4 is a long-lasting blood pool contrast agent that is slowly excreted through the kidneys (Figures 3 and 4 and Figure S25). This can be appreciated in the subtraction images shown in Figure 3B−D,F−H. It is clear that the liver and spleen showed no appreciable uptake (there

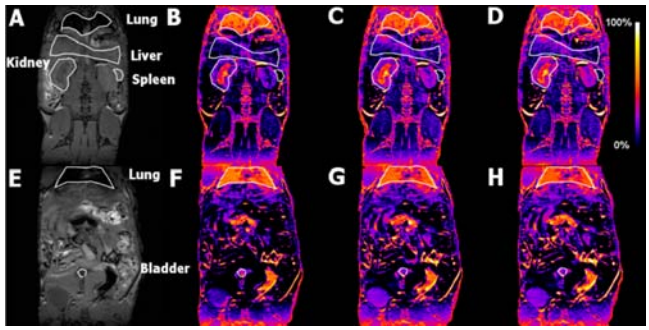

Figure 3. 3D T_1-weighted spoiled-gradient recalled-echo MRI of mouse before and after injection of **1**-mPEG-G4: (A, E) MRI before injection; (B−D, F−H) subtraction of preinjection images from images obtained (B, D) 0−30 min, (C, E) 30−60 min, and (D, H) 60−90 min after injection.

dx.doi.org/10.1021/ja3079829 | J. Am. Chem. Soc. 2012, 134, 15724−15727

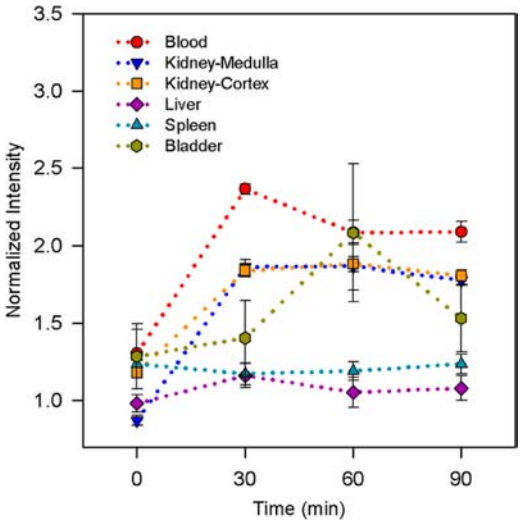

Figure 4. Plots of normalized intensities (mean ± standard error, n = 3) before and after injection of **1**-mPEG-G4.

was only a residual signal as a result of the vasculature), while the lung, normally a low-intensity organ in MRI, lightened up as a result of the enhancement of the vasculature. The MRI signal in the blood and kidneys decayed gradually, allowing for a long imaging time. For example, the image enhancements (mean ± standard deviation, n = 3) in the kidney medullas and blood vessels were 114 ± 14 and 81 ± 27% after 30 min following administration of the agent and slowly decreased to 104 ± 11 and 60 ± 26% after 90 min of scanning, respectively (Figure 4).

Although the present data did not allow for quantification of the excretion of the agent, selective uptake by the kidney medulla and cortex and the enhanced image of the bladder (Figure 3) suggest excretion of the ORCA through the kidneys. ORCA **1**-mPEG-G4, with an average number-average molecular weight (M_n) of ca. 32 kDa (Table 1), is estimated to have a Stokes–Einstein radius (r_{SE}) of ca. 2.4 nm, which is near the upper limit for glomerular filtration of positively charged spherical solutes ($r_{SE} \approx 2.5$ nm),[29] and thus could account for the strongly enhanced MR image of the kidneys, especially the medullas, over a period exceeding 1 h (Table 1).

■ ASSOCIATED CONTENT

Ⓢ Supporting Information

Materials, general methods, instrumentation, synthetic protocols, and in vitro and in vivo characterizations. This material is available free of charge via the Internet at http://pubs.acs.org.

■ AUTHOR INFORMATION

Corresponding Author

arajca1@unl.edu

Notes

The authors declare no competing financial interest.

■ ACKNOWLEDGMENTS

We thank Drs. Przemysław J. Boratyński and Krzysztof Waskiewicz for preliminary synthesis of **1**-mPEG-G4. This research was supported by NSF CHE-1012578 (UNL), NIH NIBIB EB008484 (UNL), the Nebraska Research Initiative (UNL and UNMC), and NIH NIBIB EB002807 (Denver).

■ REFERENCES

(1) Winalski, C. S.; Shortkroff, S.; Schneider, E.; Yoshioka, H.; Mulkern, R. V.; Rosen, G. M. *Osteoarthritis Cartilage* **2008**, *16*, 815.
(2) Hyodo, F.; Matsumoto, K.; Matsumoto, A.; Mitchell, J. B.; Krishna, M. C. *Cancer Res.* **2006**, *66*, 9921.
(3) Davis, R. M.; Matsumoto, S.; Bernardo, M.; Sowers, A.; Matsumoto, K.; Krishna, M. C.; Mitchell, J. B. *Free Radical Biol. Med.* **2011**, *50*, 459.
(4) Utsumi, H.; Yamada, K.; Ichikawa, K.; Sakai, K.; Kinoshita, Y.; Matsumoto, S.; Nagai, M. *Proc. Natl. Acad. Sci. U.S.A.* **2006**, *103*, 1463.
(5) Gallez, B.; Lacour, V.; Demeure, R.; Debuyst, R.; Dejehet, F.; De Keyser, J. L.; Dumont, P. *Magn. Reson. Imaging* **1994**, *12*, 61.
(6) Brasch, R. C.; London, D. A.; Wesbey, G. E.; Tozer, T. N.; Nitecki, D. E.; Williams, R. D.; Doemeny, J.; Tuck, L. D.; Lallemand, D. P. *Radiology* **1983**, *147*, 773.
(7) Braverman, I. M.; Cowper, S. *F1000 Med Rep.* **2010**, *2*, No. 84.
(8) Grobner, T. *Nephrol., Dial., Transplant.* **2006**, *21*, 1104.
(9) Marckmann, P.; Skov, L.; Rossen, D. A.; Damholt, M. B.; Heaf, J. G.; Thomsen, H. S. *J. Am. Soc. Nephrol.* **2006**, *17*, 2359.
(10) (a) Vallet, P.; Van Haverbeke, Y.; Bonnet, P. A.; Subra, G.; Chapat, J.-P.; Muller, R. N. *Magn. Reson. Med.* **1994**, *32*, 11. (b) $S = 1$ nitroxide diradicals have similarly low values of r_1 per nitroxide moiety. See: Spagnol, G.; Shiraishi, K.; Rajca, S.; Rajca, A. *Chem. Commun.* **2005**, 5047.
(11) Davis, R. M.; Sowers, A. L.; DeGraff, W.; Bernardo, M.; Thetford, A.; Krishna, M. C.; Mitchell, J. B. *Free Radical Biol. Med.* **2011**, *51*, 780.
(12) Chan, H. C.; Sun, K.; Magin, R. L.; Swartz, H. M. *Bioconjugate Chem.* **1990**, *1*, 32.
(13) Villaraza, A. J. L.; Bumb, A.; Brechbiel, M. W. *Chem. Rev.* **2010**, *110*, 2921.
(14) Floyd, W. C., III; Klemm, P. J.; Smiles, D. E.; Kohlgruber, A. C.; Pierre, V. C.; Mynar, J. L.; Fréchet, J. M. J.; Raymond, K. N. *J. Am. Chem. Soc.* **2011**, *133*, 2390.
(15) Winalski, C. S.; Shortkroff, S.; Mulkern, R. V.; Schneider, E.; Rosen, G. M. *Magn. Res. Med.* **2002**, *48*, 965.
(16) Francese, G.; Dunand, F. A.; Loosli, C.; Merbach, A. E.; Decurtins, S. *Magn. Reson. Chem.* **2003**, *41*, 81.
(17) Silberstein, T.; Mankuta, D.; Shames, A. I.; Likhtenshtein, G. I.; Meyerstein, D.; Meyerstein, N.; Saphier, O. *Arch. Gynecol. Obstet.* **2008**, *277*, 233.
(18) Keana, J. F. W.; Pou, S.; Rosen, G. M. *Magn. Reson. Med.* **1987**, *5*, 525.
(19) Vianello, F.; Momo, F.; Scarpa, M.; Rigo, A. *Magn. Reson. Imaging* **1995**, *13*, 219.
(20) Bobko, A. A.; Kirilyuk, I. A.; Grigor'ev, I. A.; Zweier, J. L.; Khramtsov, V. V. *Free Radical Biol. Med.* **2007**, *42*, 404.
(21) Kirilyuk, I. A.; Polienko, Y. F.; Krumkacheva, O. A.; Strizhakov, R. K.; Gatilov, Y. V.; Grigor'ev, I. A.; Bagryanskaya, E. G. *J. Org. Chem.* **2012**, DOI: 10.1021/jo301235j.
(22) Caravan, P. *Chem. Soc. Rev.* **2006**, *35*, 512.
(23) Joralemon, M. J.; McRae, S.; Emrick, T. *Chem. Commun.* **2010**, *46*, 1377.
(24) Sosnovsky, G.; Cai, Z. *J. Org. Chem.* **1995**, *60*, 3414.
(25) Newkome, G. R.; Moorefield, C. N.; Vögtle, F. *Dendrimers and Dendrons*; Wiley-VCH: Weinheim, Germany, 2001; pp 1–623.
(26) Sato, H.; Kathirvelu, V.; Spagnol, G.; Rajca, S.; Rajca, A.; Eaton, S. S.; Eaton, G. R. *J. Phys. Chem. B* **2008**, *112*, 2818.
(27) Nicolle, G. M.; Toth, E.; Schmitt-Willich, H.; Raduchel, B.; Merbach, A. E. *Chem.—Eur. J.* **2002**, *8*, 1040.
(28) Maliakal, A. J.; Turro, N. J.; Bosman, A. W.; Cornel, J.; Meijer, E. W. *J. Phys. Chem. A* **2003**, *107*, 8467.
(29) Haraldsson, B.; Sörensson, J. *Physiology* **2004**, *9*, 7.